Earth Surface Processes and Landforms
Earth Surf. Process. Landforms **29**, 1275–1291 (2004)
Published online in Wiley InterScience (www.interscience.wiley.com). DOI: 10.1002/esp.1094

TRACKING SEDIMENT REDISTRIBUTION IN A SMALL WATERSHED: IMPLICATIONS FOR AGRO-LANDSCAPE EVOLUTION

V. O. POLYAKOV,[1] M. A. NEARING,[2]* AND M. J. SHIPITALO[3]

[1] *USDA, ARS National Soil Erosion Research Laboratory, Purdue University, West Lafayette, Indiana, USA*
[2] *USDA, ARS Southwest Watershed Research Center, Tucson, Arizona, USA*
[3] *USDA–ARS North Appalachian Experimental Watershed, Coshocton, Ohio, USA*

Received 3 January 2003; Revised 10 October 2003; Accepted 13 February 2004

ABSTRACT

A new, multi-tracer method is used to track erosion, translocation, and redeposition of sediment in a small watershed, thus allowing for the first time a complete, spatially distributed, sediment balance to be made as a function of landscape position. A 0·68 ha watershed near Coshocton, Ohio, USA was divided into six morphological units, each tagged with one of six rare earth element oxides. Sediment translocation was evaluated by collecting run-off and by spatially sampling the soil surface. Average measured erosion rate was 6·1 t ha^{-1}, but varied between 40·4 t ha^{-1} loss from the lower channels to 24·1 t ha^{-1} gain on the toeslope. With this technique it was possible for the first time to itemize the sediment budget for landscape elements into three components: (1) the soil from the element that left the watershed with run-off; (2) soil from the element that was redeposited on lower positions, with the spatial distribution of that deposition; and (3) soil originating from the upper positions and deposited on the element, with quantification of relative source areas. The results are incongruous with the current morphology of the watershed, suggesting that diffusion-type erosion must also play a major role in defining the evolution of this landscape. Copyright © 2004 John Wiley & Sons, Ltd.

KEY WORDS: catchments; rare earth elements; run-off; sediment delivery ratio; sediment transport; soil erosion; spatial distribution of erosion; tillage erosion; tracers; watersheds

INTRODUCTION

Measurements of eroded soil are aimed at determining the gross sediment leaving an area or the spatial distribution of net amounts of soil removed or deposited. Such measurements are not capable of tracking the fate of sediment from specific source areas within the watershed. In other words, a study may show that an area on a watershed is a source area, but there has been no comprehensive way to track the redistribution of sediment from that specific area. Likewise, depositional areas may be identified, but a comprehensive method to identify the relative contributions from different source areas for the deposited sediment is not available. Thus, such measurements do not provide a full picture of sediment redistribution on a landscape.

The most common approach to studying spatial distribution of total erosion loss and gain is ^{137}Cs. Two common applications of spatial erosion data are for evaluating soil erosion models and for understanding landscape evolution processes.

Govers *et al*. (1996) evaluated a two-component soil erosion model using ^{137}Cs measurements from two, complex-shaped fields in the UK. The model consisted of a component for water erosion and a component for tillage erosion. Tillage erosion was modeled as a diffusive process, and water erosion was modeled as longitudinal flow without a diffusion component. They found that the model results best aligned with the measured spatial data when both water erosion and tillage erosion were included. In their discussions of the results, the authors stated that they thought that the diffusive processes associated with water erosion, which they considered to be limited to splash, were negligible. Several others have also used the ^{137}Cs technique for evaluating models (Rose *et al*., 1980; Ferro *et al*., 1998; Sidorchuk and Golosov, 1996; Quine, 1999; Ritchie *et al*., 1974; De Roo and Walling, 1994).

* Correspondence to: M. A. Nearing, USDA, ARS Southwest Watershed Research Center, Tucson, AZ 85719, USA.
E-mail: mnearing@tucson.ars.ag.gov

Other methods for measuring spatial distribution of erosion for purposes of evaluating models have been used. Takken *et al*. (1999) measured and mapped rill and gully volumes and thicknesses of depositional zones (sediment deposits), then used the data to evaluate the Limburg Soil Erosion Model (LISEM) model. They found that the model predicted well the sediment delivery ratio of approximately 60 per cent and zones of deposition, but did not predict spatial distribution of erosion particularly well. Apparently the model did not adequately account for the effect of vegetation differences between crops. The authors pointed out that this study illustrated the importance of using spatially distributed erosion data for testing a spatially distributed model. Even though the model was calibrated to match gross erosion rates for the area, it did not accurately reflect the relative source contributions.

A number of studies have successfully used various tracers to link hillslope geometry and position with the rate of soil loss. Daniels *et al*. (1985), using ^{137}Cs as a tracer on a watershed in North Carolina, found that severity of erosion depended on slope characteristics and topographic shape (convergence or divergence). The greatest loss occurred on the interfluve and shoulder of the slopes, moderate erosion occurred on the linear mid-slope, and slight erosion occurred on footslopes. Brown *et al*. (1981) used ^{137}Cs and found no net accumulation over a long period on footslopes, which was attributed to circulation (deposition, storage, and re-entrainment) of sediment. Montgomery *et al*. (1997) used ^{137}Cs as a tracer and found that convex backslopes and shoulder slopes experienced net loss, while concave and linear concave backslopes and footslopes experienced gain. Quine *et al*. (1997), using ^{137}Cs on a watershed in China, found that the middle portion of the slope was eroding at a greater rate than the crest, and determined that steepening of the slope was occurring as a result. Accumulation at the base of the hill was approximately equal to the rate of removal.

Other techniques have also been used to study landscape development. Olson *et al*. (2002) used fly ash deposited from the burning of coal to study soil profile depletion at different landscape positions on a cultivated field and reforested site. Deposition rich in fly ash was found on the footslope, indicating net sediment gain at that point. Fly ash as a tracer was also used by Hussain *et al*. (1998).

The ^{137}Cs and other single-tracer techniques have performed well in providing data on the spatial distribution of erosion and deposition in a study area (Ritchie and McHenry, 1990). However, a multiple-tracer technique could have a distinct advantage over the single tracer in that it may provide information on sediment redistribution. In addition to measuring the net gain at a given point on a watershed, multiple tracers can be used to identify the relative upslope source contributions of the deposited sediment at the point. Likewise, for areas of net soil loss (erosion), the fate of the lost sediment can be followed, including where the sediment was redeposited downslope and how much exited the watershed.

Recently, the feasibility of using rare earth element oxides as tracers for soil erosion studies has been evaluated by examining their binding ability with soil materials (Zhang *et al*., 2001). Five rare earth element oxide powders were mixed with a silt loam soil and leached with deionized water to evaluate the mobility of the elements. The study indicated that the rare earth element oxides were uniformly incorporated into soil aggregates of different sizes and that direct mixing of a trace amount of rare earth elements apparently did not substantially alter physicochemical properties of soil particles and aggregates.

Studies using a suite of rare earth elements under rainfall simulation have further confirmed the feasibility of using rare earth element oxides as a sediment tracer (Zhang *et al*., 2003; Polyakov and Nearing, 2004). In both studies a suite of five rare earth element oxides were mixed with a silt loam soil, which was placed in a 4×4 m soil box with one element at each of five slope positions in the box (in strips from upper to lower end). Rainfall of 60–90 mm h^{-1} was applied. Erosion rates for different slope positions estimated from rare earth element concentrations correlated well with those calculated from the laser-scanned DEMs.

The objectives of this study were to apply the rare earth element method to a small watershed to assess its applicability under field conditions and to evaluate the spatial redistribution of sediment within the watershed. This study provides data of a kind never before reported. For the first time we utilize a method to track erosion, translocation, and redeposition of sediment in a small watershed, thus allowing a complete, spatially distributed, sediment balance to be made as a function of morphological landscape elements. The sediment budget for each landscape element was divided into three components: (1) the soil from the element that left the watershed with run-off; (2) soil from the element that was redeposited on lower positions, with the spatial distribution of that deposition; and (3) soil originating from the upper positions and deposited on the element, with quantification of relative source areas.

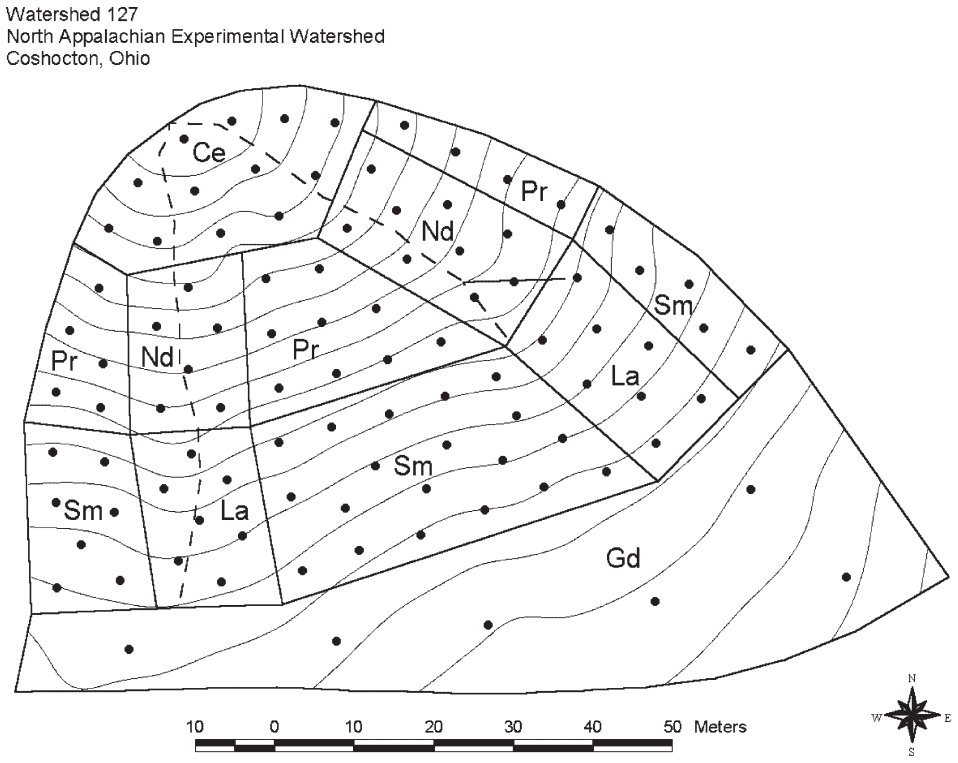

Figure 1. Topography, location of channels, and location of surface sampling points on the experimental watershed. The elementary morphological units are delineated by polygons and labeled with the corresponding rare earth element name: toeslope (Ce), lower (Pr) and upper (Sm) backslopes, lower (Nd) and upper (La) channels, and shoulder (Gd). Contour intervals are 0·5 m

MATERIALS AND METHODS

Description of the experimental site

The experiment was conducted at the North Appalachian Experimental Watershed, located within the unglaciated Allegheny portion of the Appalachian Plateau. The site is in Coshocton County, Ohio, approximately 15 km northeast of the city of Coshocton (40°22′ N and 81°48′ W) (Kelley *et al*., 1975).

Watershed 127, selected for the study, has an area of 0·68 ha with maximum length of 125 m and slopes ranging between 1° and 12° (Figure 1). The watershed has three distinct geomorphic components: the shoulders with gradients less than 5°, the backslopes with gradients ranging from 5° to 12°, and the toeslopes ranging from 1° to 3°. A nose slope near the center of the watershed divides the watershed into two approximately equal parts with two distinctive channels. The total range of relief on the watershed is approximately 9 m. The watershed outlet is equipped with H flume with a flow-proportional Coshocton Wheel sampler (Brakensiek *et al*., 1979).

A survey of the area was conducted using a transit. Over 200 elevation points collected during the survey were interpolated into a raster DEM with 0·2 m grid size, using the regularized spline method in ArcView 3.1 (Figure 1).

Soils, climate, and management on the experimental watershed

Soils of the watershed developed in interbedded clay shales and sandstone bedrock and were represented by three soil series: Keene, Coshocton-Rayne, and Clarksburg. The Keene silt loam (fine-silty, mixed, mesic Aquic Hapludalf) at the top of the slope grades into the Coshocton-Rayne silt loam (fine-loamy, mixed, active, mesic Typic Hapludult) on the middle, and the Clarksburg silt loam (fine-loamy, mixed, superactive, mesic Oxyaquic Fragiudalf) found at the toeslope. The average annual precipitation is 940 mm.

Table I. Amount of tracers used, background concentrations, applied concentrations, and their areas of application in Watershed 127

	Unit	REE tracer					
		La	Ce	Pr	Nd	Sm	Gd
Application section[a]		UC	TS	LBS	LC	UBS	SH
Application area	m^2	741	550	904	717	1545	2300
Fraction of area	%	11·0	8·1	13·4	10·6	22·9	34·0
Mass of oxide applied	kg	14·8	34·8	6·1	12·1	5·6	11·0
Background concentration	mg kg^{-1}	13·7	33·4	3·6	14·9	2·8	2·5
Target concentration[b]	mg kg^{-1}	177	526	57	152	32	42
Measured concentration[c]	mg kg^{-1}	239	773	81	223	49	48

[a] UC, upper channel; TS, toeslope; LBS, lower backslope; LC, lower channel; UBC, upper backslope; SH, shoulder.
[b] Target concentration determined assuming uniform mixing to a depth of 8 cm.
[c] Measured concentration is average of 11–56 samples, depending on size of application area, taken after tracer application.

The watershed was disked using light equipment to a depth of approximately 8 cm once on April 30, once on May 1, twice on May 3, four times on May 4 and once on May 10, 2001. Normally the watershed is disked three to four times before planting, but in 2001 it was disked more intensively to smooth the surface for tracer application and, afterwards, to incorporate the applied tracer. The watershed was planted to soybean on May 11, 2001 at a spacing of 76 cm with rows along the contour. The crop was harvested on October 9th, 2001.

Rare earth element properties, preparation, and application

Six rare earth element oxides (La_2O_3, Pr_6O_{11}, Sm_2O_3, Gd_2O_3, Nd_2O_3, and CeO_2) were used. The watershed was divided into six morphological units to provide association between topography and erosion (Figure 1). Consideration for the division were the flow accumulation pattern, slope gradient and aspect, and observations in the field such as existing rills, depositional areas, etc. The watershed was subdivided into toeslope, backslope, shoulder, and channels. Backslopes and channels were divided into upper and lower parts. A different tracer element was assigned to each morphological unit.

The rare earth element oxide powders were thoroughly mixed with air-dry soil in an approximate proportion of 1:10, then wetted and air-dried again. The wetting and drying cycle was meant to better associate the tracer powder and soil aggregates. The mixture of rare earth element and soil was spread on the watershed on May 2, 2001 using a calibrated 56 cm-wide lawn spreader modified with heavier wheels and weights.

Amount of tracers used and the area of application are given in Table I. The target concentration of added tracer was 10–17 times the background concentrations of the elements, assuming an incorporation depth of 8 cm. After each morphological unit was marked with its unique tracer, the area was lightly disked as reported above.

Sample collection

Soil surface samples and run-off samples were collected during the course of the experiment. Run-off samples were used to determine the total sediment yield from the watershed and from each morphological unit. Surface samples were used to quantify and identify by source the sediment deposition on the watershed. Surface sample locations were uniformly distributed over the area, except for the shoulder section, which was sampled less extensively (Figure 1). This was done because the shoulder area occupied the uppermost location on the watershed and no deposition from other sections was expected. Locations of the sampling points were determined such that no two were closer than 6 m apart. A total of 94 sample locations were triangulated on the field and marked with flags. Each combined sample consisted of 30 subsamples taken randomly within a distance of 2 m from the flag to a depth of 3 cm using a metal probe 14·5 mm in diameter. Surface samples were collected on June 17 and November 8, 2001.

Run-off samples from the watershed were collected during each rainfall event and consisted of two parts: sediment obtained from a tank into which run-off was routed; and from the flume floor. Run-off in the tank was a flow-proportional composite sample obtained using a Coshocton Wheel sampler (Brakensiek *et al*., 1979). Sediment from the flume floor was the sediment that left the watershed during the event, but was deposited on the floor of the flume before reaching the Coshocton Wheel sampler. These two fractions were summed to determine total amount of soil that left the watershed, but analyzed separately for rare earth element concentrations. Soil samples were air-dried, thoroughly mixed, and ground. Subsamples of 2 g were taken for acid digestion and analysis by inductively coupled plasma mass spectrometer (ICPMS). Volume of run-off was measured using a water stage recorder in the outlet flume.

Rare earth element extraction and analysis

Samples were prepared for ICPMS analysis using the extraction procedure modified by Zhang *et al*. (2001) from USEPA standard method for extractions of metals from environmental samples (USEPA, 1995). Two grams of soil sample was placed into a 50 mL flask. Ten milliliters of concentrated HNO_3 (70 per cent by weight) was added, and the mixture refluxed for 2 h in a water bath at 85 °C. After cooling to less than 70 °C, 10 mL of H_2O_2 (30 per cent) was slowly added to remove organically bound rare earth elements. The solution was then brought to 85 °C until effervescence subsided. Five milliliters of concentrated HCl (36 per cent by weight) was added, and the solution again refluxed for 2 h in a water bath at 85 °C. After a 24 h waiting period at room temperature, the solution was filtered through Whatman filter paper #5, and eluted with 5 mL DW (18 MΩ cm^{-1}). The solution was then filtered through a 0·45 μm membrane.

Analyses for the rare earth elements were performed in the Center for Trace Analysis, Department of Marine Science, University of Southern Mississippi. Samples were diluted 1000–10 000-fold in 1 per cent nitric acid with 2 ppb of In. Instrumentation used was ThermoFinnigan Element 2 Sector Field ICP-MS and Cetac Aridis desolvating nebulizer. Estimated detection limit was 0·03 mg kg^{-1} with estimated precision ±5 per cent.

Data obtained from chemical analysis of on-site and run-off soil samples were used to determine patterns of soil particle movement and to locate sources and sinks of sediment. Concentrations of tracers in samples were compared to the background and application levels. Increased concentration of tracer in the surface samples indicated depositional areas or sinks, while such an increase in the run-off samples indicated that the area labeled with corresponding tracer was the sediment source.

The proportional method used in the analysis is based on the assumption that the concentration of the tracer in bulk soil is equal to the concentration of that in the eroding soil:

$$L_i = L_t(C_{mi} - C_{bi})/(C_{ai} - C_{bi}) \tag{1}$$

where L_i(g m^{-2}) is the soil loss from area with *i*th tracer, L_t(g m^{-2}) is the total soil loss, C_{mi}(g g^{-1}) is the measured tracer concentration in sediment yield, C_{bi}(g g^{-1}) is the background concentration, and C_{ai}(g g^{-1}) is the application concentration. Some sediment after detachment was redeposited on the lower part of the watershed. Soil movement on the slope can be accounted for by analyzing the surface samples using

$$D_i = (m/A) \times (C_{mi} - C_{bi})/(C_{ai} - C_{bi}) \tag{2}$$

where D_i(g m^{-2}) is the deposition of sediment tagged with *i*th tracer, m(g) is the mass of the sample, and A(m^{-2}) is the area of the sample.

Geostatistical analysis

ArcView GIS 3.2 (ESRI, 1999), and GS^+ 5.1.1 (Gamma Design Software, 2000) programs were used to perform interpolations and spatial analyses. A regularized spline interpolation method was used to produce a DEM of watershed topography. Maps of erosion and sediment accumulation on the watershed were prepared using an ordinary block kriging method.

Table II. Characteristics of rainfall events that occurred on Watershed 127 during the course of the experiment, run-off from the watershed, and measured soil loss. (Rainfall was recorded at the gage no. RY103)

Rainfall event	Precipitation[a]		Run-off		Sediment yield (kg)
	Total (mm)	Peak (mm h^{-1})	Total (mm)	Peak (mm h^{-1})	
May 21	29·5	189·0	8·3	54·8	1290
May 22	17·3	46·0	7·4	9·8	60
June 2	12·4	56·0	2·2	5·2	30
June 6	8·1	27·0	trace	0·0	–
June 15	16·3	114·0	0·1	0·7	–
July 25	90·2	114·0	44·9	102·4	2760
August 9	19·3	173·0	0·1	0·6	–
August 31	24·1	59·0	0·1	1·2	–
Other	113·5	–	–	–	–
Total	301·2		63·1		4140

[a] Rainfall was recorded at gage no. RY103.

RESULTS AND DISCUSSION

Rainfall events and soil loss

The total amount of precipitation during the experiment was 300 mm, 20 per cent of which left the watershed as run-off. Average annual rainfall at the location for the period from 1937 through 2002 was 950 mm. The two largest events of May 21 and July 25 produced 98 per cent of the total sediment during the experimental period (Table II). They were both short-duration, high-intensity storms (Figure 2) with 29·5 and 90·2 mm of precipitation respectively, of which 26·7 mm and 77·8 mm were delivered at intensities of over 25 mm h^{-1}. These storms represent 24 h return frequencies of under one year and approximately eight years, respectively.

Variability of rare earth element concentrations in soil samples

The precision of soil deposition measurements by a tracer depends on how accurately the tracer's concentration and its background in the soil can be measured. For example, for ^{137}Ce, the most commonly used soil tracer, the median coefficient of variation (CV) of its activity on undisturbed soil reported in the literature, as cited by Sutherland (1994), was 19·3 per cent. Such variability makes detecting soil loss over short periods of time and on an event basis almost impossible. The CV of rare earth element background concentrations in our study ranged from 4·5 per cent for Sm to 9·8 per cent for Gd. On average, 10 independent random samples were needed to estimate the background level of a rare earth element in soil with an allowable error of 5 per cent at 95 per cent confidence.

To measure the amount of sediment deposition, the proportional method (Equation 2) uses the ratio of tracer concentration change measured in the location of interest to the concentration of tracer application. This makes the result sensitive to an accurate estimation of the tracer background value. Soil movement may be statistically detected if an increase in rare earth element concentration exceeded the 95 per cent confidence limit for the background value. The confidence limit for the mean value depends on the number of samples, and in our study the minimum threshold of sedimentation detection for La, Pr, Nd, Sm, and Gd tracers was 0·3, 0·2, 0·4, 0·7, and 1 t ha^{-1}, respectively. Details of the calculations for these limits were presented by Polyakov (2002).

Obviously, the ability to detect sediment (either deposited or in run-off) from a given source area is also dependent upon the level of application of the tracer, since a smaller amount of sediment would be required to exceed the confidence interval limits of the background levels for a given tracer if the added tracer is applied at a more concentrated level.

The actual concentrations of applied tracers within their respective areas of application were somewhat higher than targeted levels (Table I), and were between 15 and 23 times the background levels. This was probably due

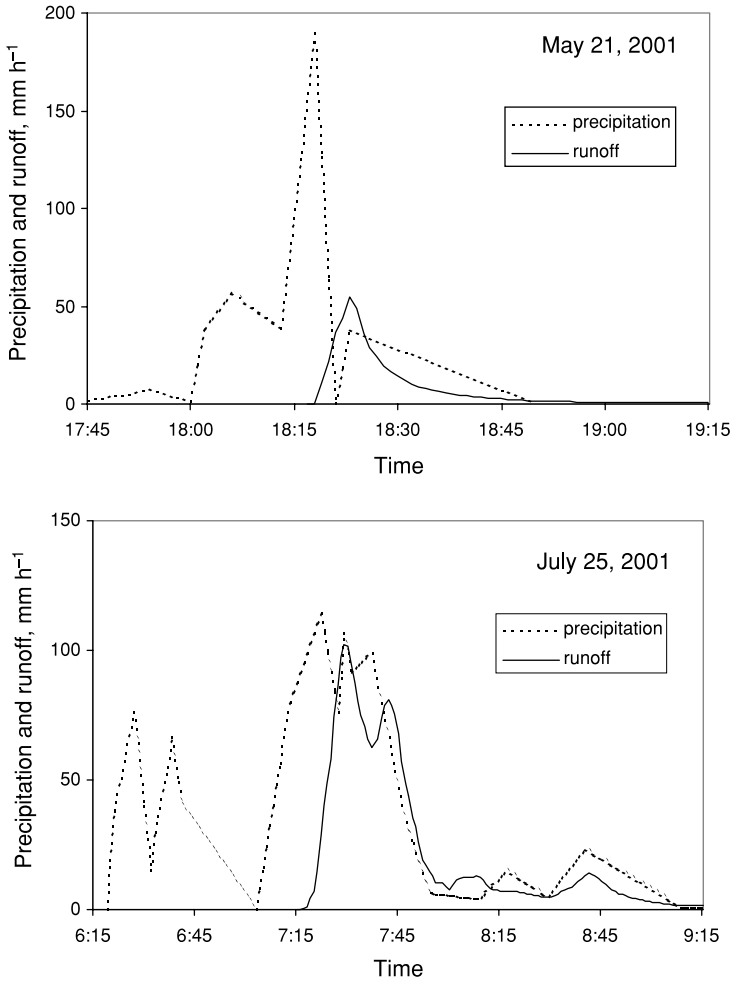

Figure 2. Precipitation pattern and hydrographs of the two largest rainfall events that occurred during the study

to the fact that incorporation depth was less than the targeted 8 cm. This may have caused some problems in measurement and interpretation of erosion where rill depths exceeded the depth of tracer incorporation. Although in general most of the rills observed after the flows were relatively wide and shallow, there was undoubtedly some mixing of unlabeled soil with the labeled soil in the measured sediment. The extent of this error was not analyzed in these results.

Soil movement on the watershed

The results of this study showed details of depositional patterns from several of the landscape elements on downslope areas (Figures 3–6). This is the first time that data has been collected that allows differentiation of sediment sources over an entire watershed area, and the patterns are striking. In general, deposited sediment from a given source area either moves only a short distance to adjacent areas or is transported through the channel system to the toeslope. The pattern is particularly clear for the shoulder slope area (Gd tracer), where there is a wide depositional area just below the shoulder slope, followed by a nearly complete absence of the tracer until additional deposition is observed on the toeslope (Figure 6). A similar pattern is observed for the upper slope and upper channel areas (Figures 4 and 5). The probable reason for this is related to the processes of erosion. Deposition near the source area is probably due to tillage erosion caused by the diskings done during the experiment and to splash and thin sheet flow (i.e., interrill erosion), in which cases the distances of sediment

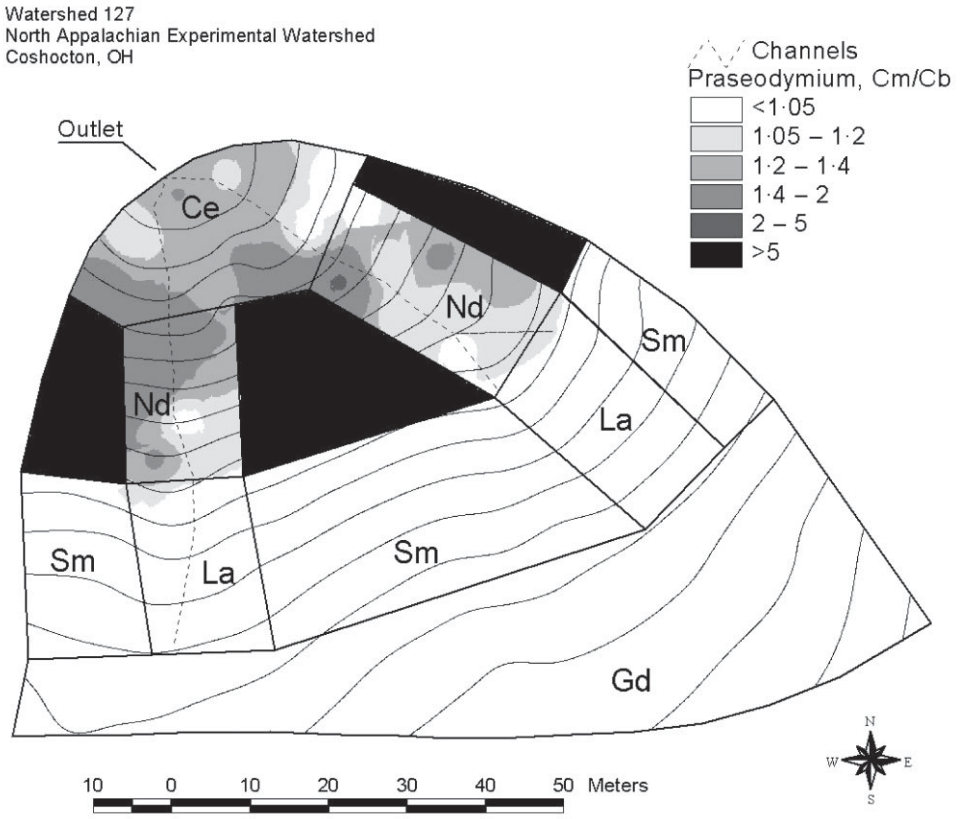

Figure 3. Redistribution of Pr tracer from the area of its application (lower backslope) to the areas downslope by November 8, 2001. Cm/Cb is the ratio of the background concentration to measured concentration. Contour intervals are 0·5 m

movement would have been relatively short. Sediment that is entrained in the flow of large rills and channels will move relatively unfettered down the watershed to be either deposited on the toeslope or to leave the watershed outlet. These results have important implications for understanding the morphologic evolution of hillslopes and for developing erosion models.

Because we did not measure the spatial distribution of the tracer on the watershed after tillage and prior to rainfall, we have no measurable way to differentiate the relative contributions of tillage or water erosion to the diffusive, or short-distance, movement that was observed in this watershed. All we can do is look at the spatial patterns that were observed in the data. Tillage was done in an east–west direction over the entire watershed, parallel to the south watershed boundary on its western half. The tillage was done with a shallow disk. Based on previous studies of tillage erosion, dislocation of soil would be expected to occur in the direction of and perpendicular to the tillage direction (Van Muysen and Govers, 2002; Van Oost *et al*., 2003). If some of the diffusion were caused by water erosion, the direction would be downslope if caused by splash, or in the direction of water movement if caused by sheet flow.

Govers *et al*. (1996) considered the potential diffusive processes for a study site in the UK, and through modeling techniques concluded that splash erosion and soil creep could explain only a small portion of the magnitude of diffusion observed in the experimental study. Thus we did not expect that the contribution of water to diffusion would be important in this study. Indeed, many of the diffusive transport patterns are explainable by tillage erosion. Figures 3 and 4 show the displacement of the soil from the hillslopes to the neighboring channel regions, which were basically in the direction of the tillage (east–west). The literature on tillage erosion suggests that tillage is anisotropic, with a greater movement in the direction of the tillage pass (Van Muysen and Govers, 2002; Van Oost *et al*., 2003).

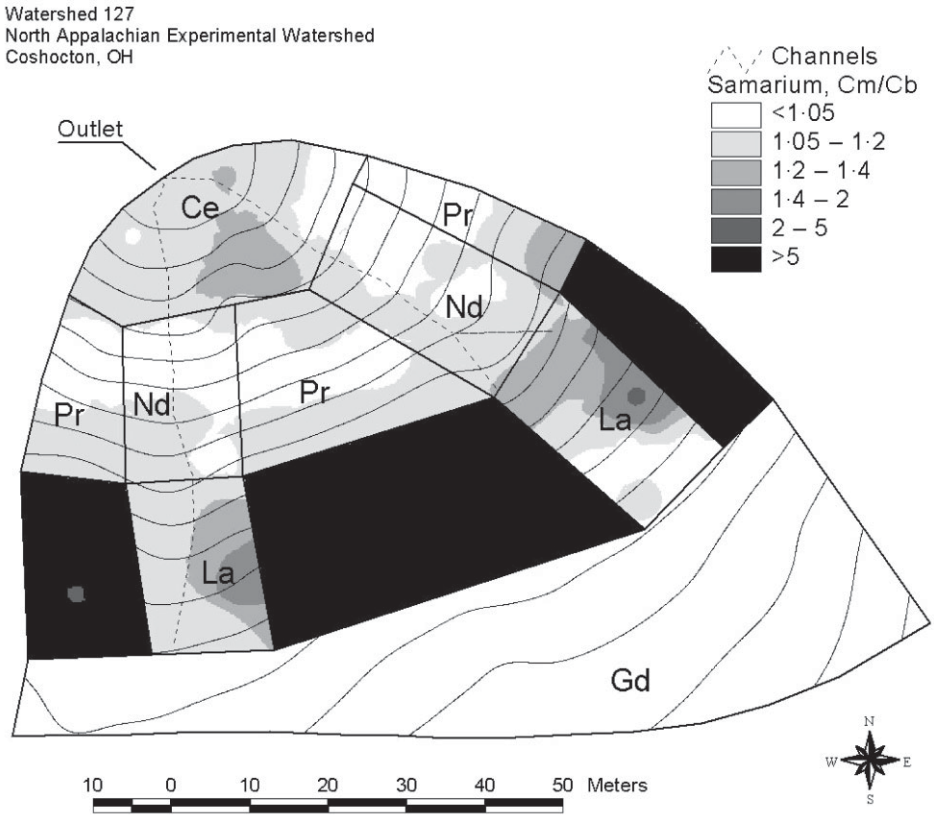

Figure 4. Redistribution of Sm tracer from the area of its application (upper backslope) to the areas downslope by November 8, 2001. Cm/Cb is the ratio of the background concentration to measured concentration. Contour intervals are 0·5 m

However, an argument can be made that diffusive erosion by water was active, also. In particular, note that the tillage direction from the eastern upper channel area (Figure 5) would have been, on its western boundary, in the cross-slope, but somewhat downslope, direction. (These were not incised channels in this field.) Yet there was no apparent lateral movement of sediment observable in the depositional patterns from those areas to the adjacent hillslope areas. The predominant flow direction from the upper channels would have been downslope to the lower channels, which was also the direction of the diffusive soil movement. In the case of the eastern upper channel, the deposition immediately down-channel (to the northwest) could have been brought into that position by tillage across the northwest boundary of the upper channel area. But if this were the case, then the La tracer from the upper channel should also have been detected in the central, upper hillslope area along its eastern border with the La (upper channel) area. The patterns shown in Figure 5 are difficult to explain via the argument of tillage erosion alone.

If a portion of the depositional patterns indicating diffusive soil movement were caused by water erosion, one possible explanation may be that the previous work in delineating diffusive erosion mechanisms has relied largely on models that only consider splash. Another possibility is that soil dislodged by splash is moving as sediment in thin sheet flows over short distances without being entrained in rills and carried long distances downslope.

Note that the types of interpretations we presented for Figures 3–6 for deposition of individual tracers are not possible when interpreting total deposition distributions (Figure 7). Such maps of total deposition are similar to what one might obtain from a single tracer study, such as ^{137}Cs, though on a different time-scale. The spatial distribution from Figure 7 is essentially a result of two individual storms, whereas ^{137}Cs results are integrations over multiple decades of erosion.

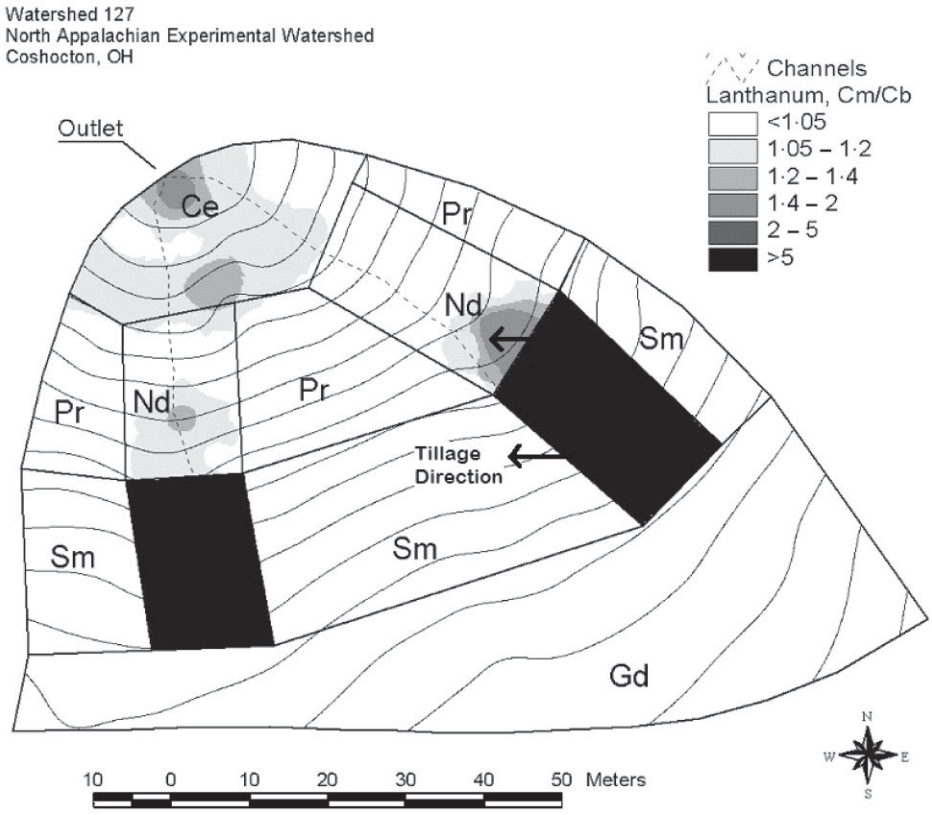

Figure 5. Redistribution of La tracer from the area of its application (upper channel) to the areas downslope by November 8, 2001. Cm/Cb is the ratio of the background concentration to measured concentration. Contour intervals are 0·5 m

The topography of the watershed gives an insight into the spatial distribution of the total soil deposition. Doubly convex hillslopes are generally characterized by the lowest sediment retention rates compared to other landscape components, while doubly concave areas with convergent flow often become sediment sinks (Montgomery *et al*., 1997). This trend corresponds well with the sedimentation pattern derived from rare earth element tracer analysis. Local accumulation of sediment coincided with the slope gradient decrease or concave forms of relief (Figure 7). Channels and toeslope were sites of deposition, accumulating 7·9 and 25·8 t ha^{-1} respectively by November 8, while somewhat less sediment was retained on the upper and lower backslopes (1·3 and 6·6 t ha^{-1}) (Table III).

Sediment yield from individual topographic elements of the watershed during the storms on May 21 and August 25, as determined from the concentration of a specific rare earth element in the run-off samples, reveals a relationship between the magnitude of soil loss and flow accumulation (Figure 8). The combined sediment yield caused by these two storms was the greatest on the lower channels (31·5 t ha^{-1}). Interestingly, the channels were also sites of considerable deposition (Figure 7), indicating that a large turnover of soil was occurring there. Sediment yield from other locations was moderate and varied between 8·8 t ha^{-1} from the upper channels and 1·6 t ha^{-1} from the shoulder slope. The upper backslope, characterized by divergent flow, had a relatively small sediment yield (2·7 t ha^{-1}).

Despite a considerable flow concentration on the toeslope, sediment yield from there was only 1·7 t ha^{-1}. A possible explanation for this is that, near the outlet, flow from the upper watershed elements was channeled into major rills, while most of the toeslope area had low flow concentration and, as a result, a low erosion rate. Also, as the slope gradient decreased, a large amount of sediment being carried from the upper sections was deposited, thus shielding the original soil on the toeslope. Visual observations of sediment deposition on the watershed

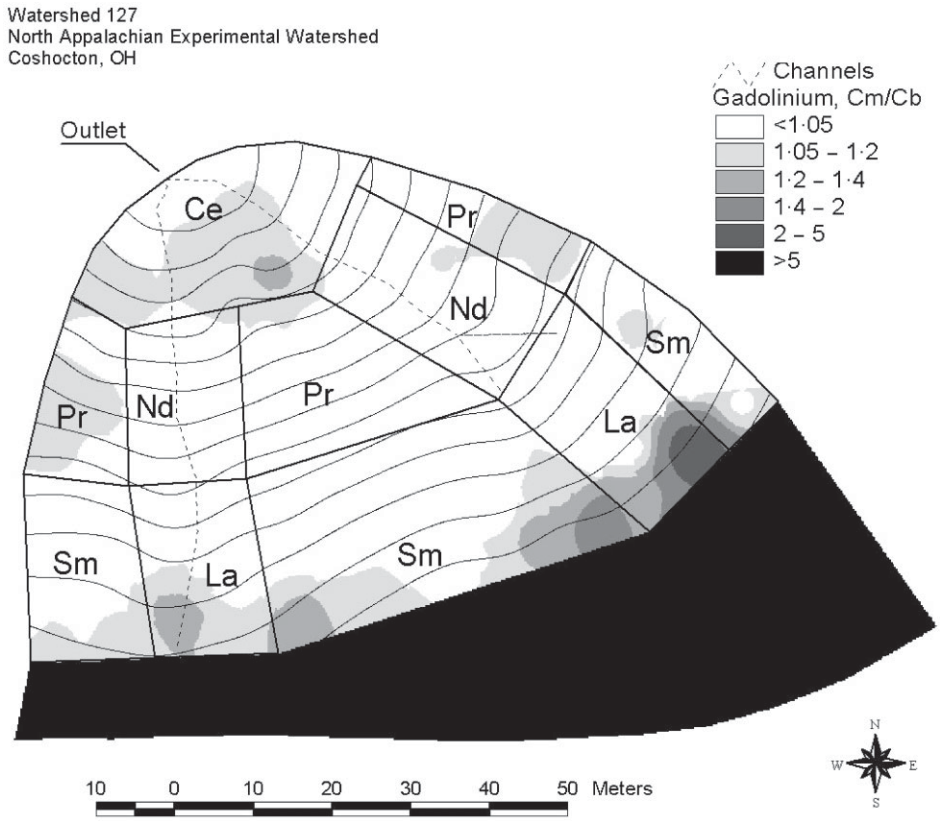

Figure 6. Redistribution of Gd tracer from the area of its application (shoulder slope) to the areas downslope by November 8, 2001. Cm/Cb is the ratio of the background concentration to measured concentration. Contour intervals are 0·5 m

Table III. Sediment deposition on the watershed for July 17 and November 8, 2001 as determined from the surface samples

Sediment deposited to:	Sediment originated from:					
	Backslope, lower	Channel, lower	Backslope, upper	Channel, upper	Shoulder slope	Total
			(t ha^{-1})			
June 17						
Toeslope	3·8	17·6	3·4	2·6	2·5	29·9
Backslope, lower	–	0·8	1·0	0·2	0·2	2·2
Channel, lower	1·4	–	0·3	1·6	1·8	5·1
Backslope, upper	–	–	–	0·1	0·9	1·0
Channel, upper	–	–	2.2	–	1·5	3·7
November 8						
Toeslope	4·3	14·6	3·1	2·2	1·5	25·8
Backslope, lower	–	4·1	1·6	0·2	0·6	6·6
Channel, lower	4·4	–	1·5	1·7	0·3	7·8
Backslope, upper	–	–	–	0·3	1·1	1·3
Channel, upper	–	–	4·9	–	3·1	8·0

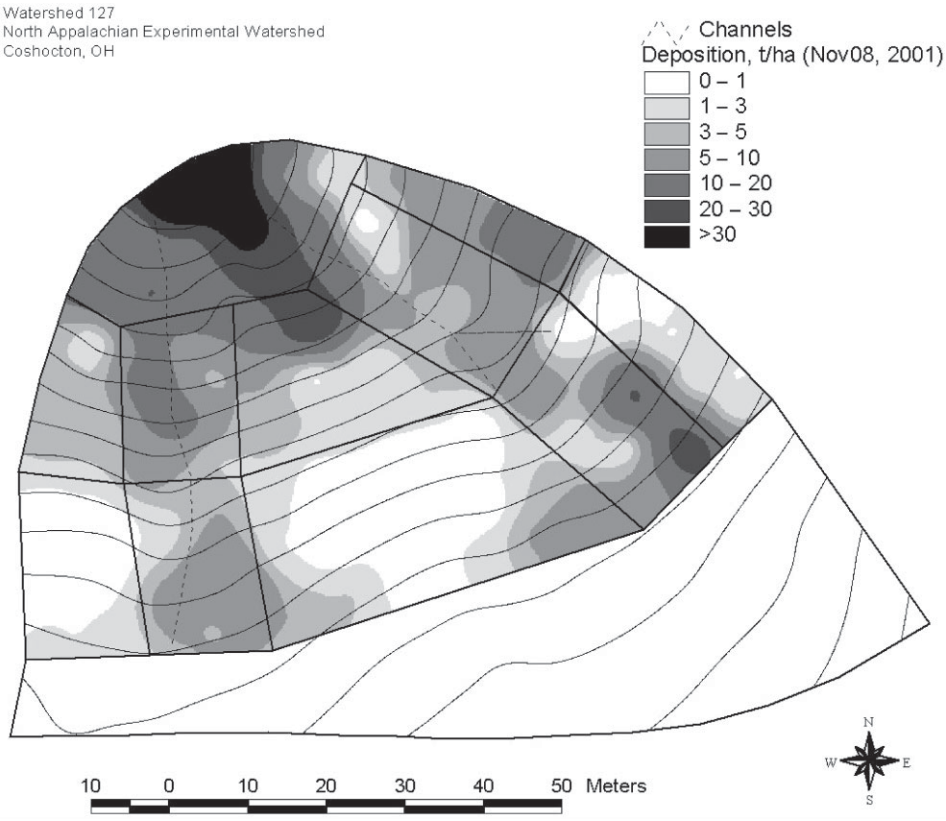

Figure 7. Sediment deposition on the watershed by November 08, 2001 as determined from the surface samples. Contour intervals are 0·5 m

toeslope area after the May 21 storm also support this suggestion. Two large rills converged next to the outlet where the slope gradient was less than 3 per cent, and an alluvial fan covered the lower portion of the toeslope area reaching a depth of several centimeters.

It is important to note in interpreting the results of Figures 8–10 that four of the morphological units (lower and upper channels, and lower and upper hillslopes) have two or three spatial samples on which the same tracer type is used. This implies that it is not possible to differentiate between the two or three locations (e.g., between the two upper channel segments) and that the sediment balance for those two were the lumped together.

Soil budget and its dynamics

The sediment budget for a specific location on the watershed consists of three components: (1) the soil from the element that left the watershed with run-off; (2) soil from the element that was redeposited on lower positions; and (3) soil originating from the upper positions and deposited on the element. The sediment yield was calculated using the run-off samples and could be determined only as an average for the area where the tracer was applied. In other words, the spatial resolution of the sediment yield data was equal to the size of the elementary watershed units. Deposition data were obtained using surface samples, and, thus, had a spatial resolution greater than that of sediment yield data. Thus, to calculate the sediment balance, the deposition data were averaged over the corresponding watershed element and combined with the sediment yield data.

During the time between the beginning of the experiment and both June 17 and November 8, all parts of the watershed, except for the toeslope, experienced a net loss of soil (Figures 9 and 10). By the end of the experiment (November 8) the average balance from the entire watershed was $-6{\cdot}1$ t ha^{-1} ($4{\cdot}14$ t over $0{\cdot}68$ ha). However, the balance on individual landscape elements ranged from a loss of $40{\cdot}4$ t ha^{-1} from the lower channels to a gain of $24{\cdot}1$ t ha^{-1} on the toeslope.

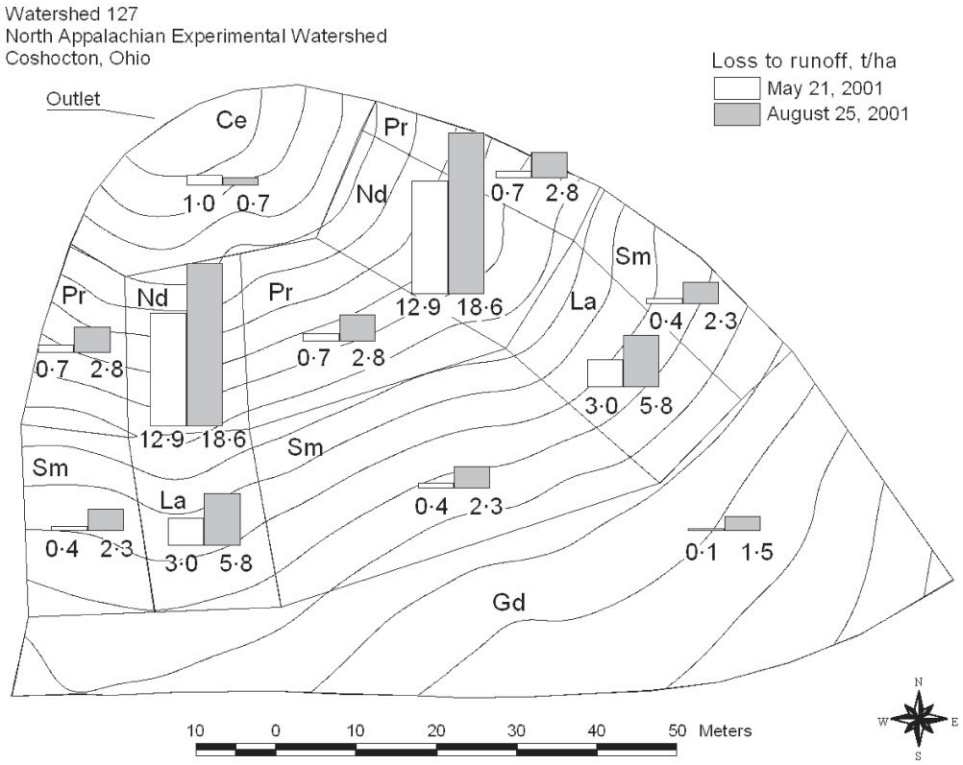

Figure 8. Soil loss to run-off from various landscape elements of the watershed during May 21 and August 25 storms as determined from the run-off samples. Contour intervals are 0·5 m

The sediment delivery ratio is defined as the ratio of sediment yield to the total amount of sediment eroded from the location under study (sediment yield plus redeposition). Spatial and temporal patterns for sediment delivery ratio are evident in the data (Table IV). Spatially, the channels showed a higher sediment delivery ratio than did the backslopes and shoulder. This, again, is related to the high sediment transport efficiency in the channels as compared to the slopes. Temporally, we see an increase in the measured sediment delivery ratio from the first to the second sediment balance computation. Overall sediment delivery was 24·1 per cent on June 17, but increased to 48·8 per cent by November 8. While cumulative sediment yield from the watershed more than tripled from the June 17 to November 8 sediment balance (from 2·0 to 6·1 t ha^{-1}), the amount of redeposited sediment increased on average by only 28 per cent (from 3·9 to 5·0 t ha^{-1}). On the toeslope deposited sediment even decreased (Table IV).

We hypothesize that the sediment delivery ratio, as measured by this method, would increase toward a quasi-equilibrium value in time, as the continuous process of redeposition and re-entrainment of soil particles also maintains a quasi-equilibrium condition. While the cumulative amount of soil reaching the outlet increases with every storm event, the amount of sediment in transition (temporarily redeposited) should remain relatively stable.

Limitations of the technology

This method of sediment tracing provides us with a new and powerful technique for measuring sediment redistribution in watersheds; however, it is not without its limitations. The method in its current form requires the mixing of the tracer into the soil profile, in this case by disking. This may limit its full applicability from natural areas or no-till fields that cannot be tilled without severe disturbance of the system to be tested. Also, the method requires a considerable amount of time and expense compared to other methods, such as the use of ^{137}Cs. The rare earth materials themselves are expensive, and measurement of rare earth concentrations are time

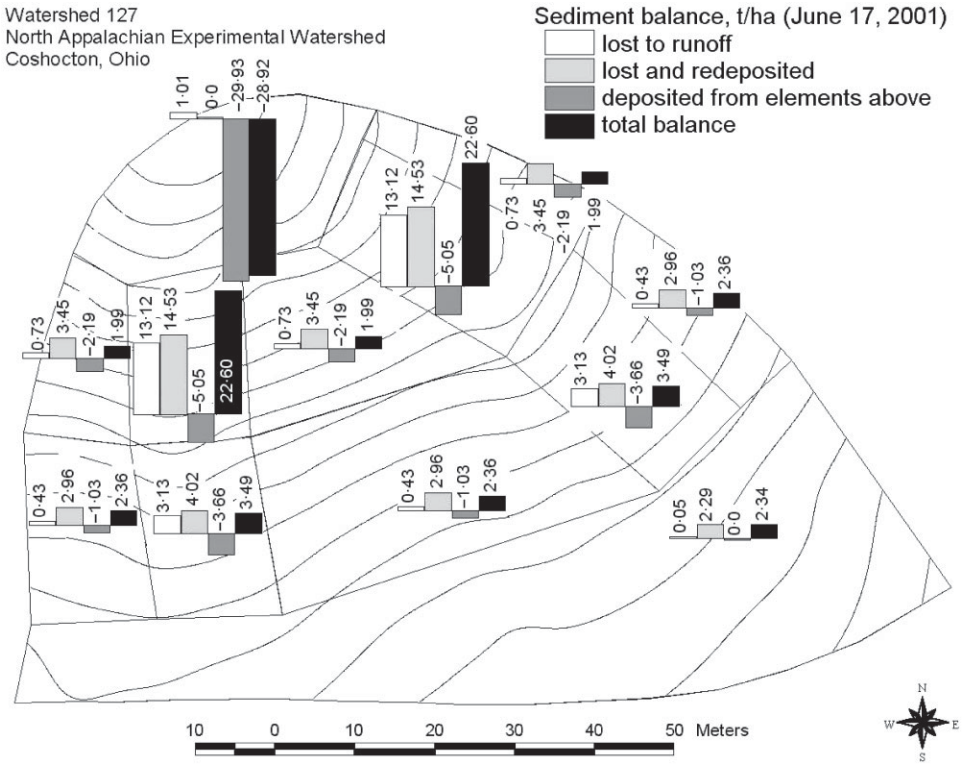

Figure 9. Sediment balance on the watershed by June 17, 2001. Contour intervals are 0·5 m

Table IV. Sediment balance for the watershed and its morphological elements as of June 17 and November 8, 2001

	Watershed element						Area weighted average
	Toeslope	Backslope		Channel		Shoulder	
		Lower	Upper	Lower	Upper		
	(t ha^{-1})						
June 17							
Loss to runoff	−1·0	−0·7	−0·4	−13·1	−3·1	−0·1	−2·0
Lost and redeposited	−0·0	−3·5	−3·0	−14·5	−4·0	−2·3	−3·9
Depositional gain	29·9	2·2	1·0	5·1	3·7	0·0	3·9
Balance	28·9	−2·0	−2·4	−22·6	−3·5	−2·4	−2·0
Sediment delivery, %	100·0	17·4	12·8	47·5	43·8	2·5	24·1
November 8							
Loss to runoff	−1·7	−3·6	−2·8	−31·8	−8·9	−1·6	−6·1
Lost and redeposited	−0·0	−6·1	−5·1	−16·4	−4·1	−2·4	−5·0
Depositional gain	25·8	6·6	1·3	7·8	8·0	0·0	5·0
Balance	24·1	−3·1	−6·5	−40·4	−5·1	−4·0	−6·1
Sediment delivery, %	100·0	36·7	35·3	65·9	68·6	38·8	48·8

consuming and expensive. Also, it is relatively difficult to interpret the influence of erosion in rills or channels when the eroded depth exceeds the incorporation depth of the tracer.

In this study we did not test the uniformity of the original mixing of the tracer within the soil over the watershed. Our assumption was that we were sampling patterns of erosion over areas that were relatively large

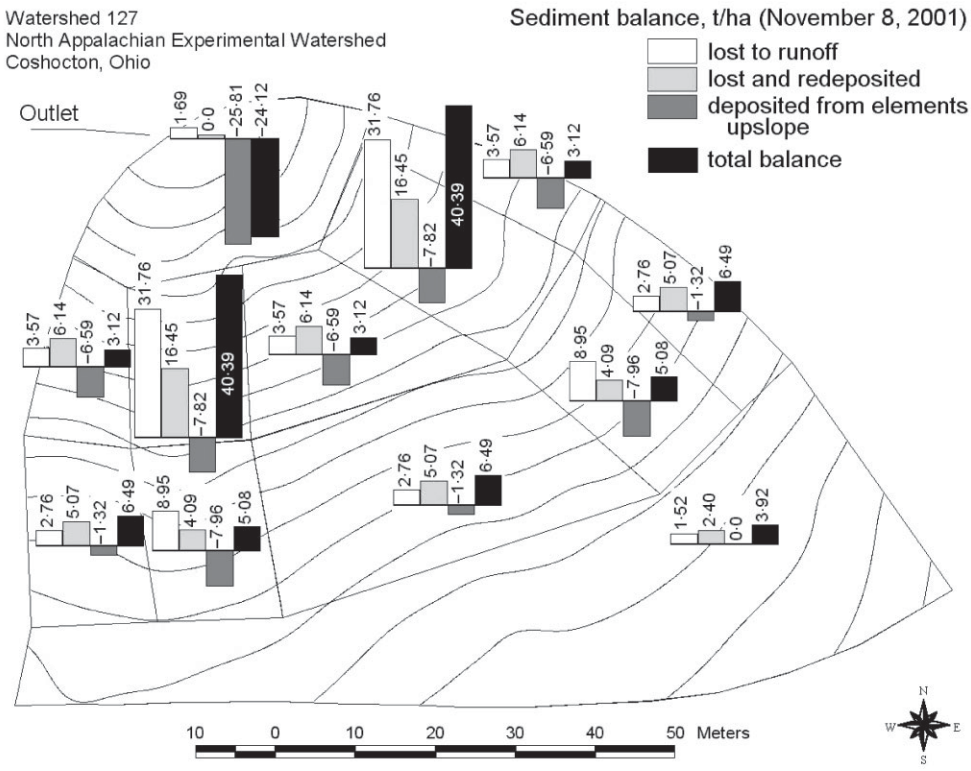

Figure 10. Sediment balance on the watershed by November 8, 2001. Contour intervals are 0·5 m

compared to the variability. As mentioned in the 'materials and methods' section, 30 subsamples were taken randomly within a 2 m radius of the sample point and integrated for measurement. It would be useful in future studies to validate that assumption with spatial measurements of the tracer immediately after its application.

Implications

Both channels and backslopes were located on the middle part of the watershed, which was eroding at a greater rate compared to the crest and the toeslope. We hypothesize that such a process would lead to steepening of the watershed's middle slopes and the formation of a more concave profile over a long period of time. Quine *et al*. (1997), observing an increased soil loss rate on the backslopes on a watershed in China, arrived at a similar conclusion. According to Penck's theory (Penck, 1924), concave slopes are characteristic for landscapes with low to medium relief.

The data point out two distinct processes of landscape development occurring simultaneously due to a combination of tillage and water erosion process. One is associated with the longitudinal erosion in the channels, where the greatest sediment yield rates were observed in this experiment (Figure 8). These data would support the back-cutting hypothesis of Penck (1924) for describing landscape evolution. However, a secondary process of tillage and/or sheet erosion in also evident in the tracer-specific deposition data (Figures 3–6). This data coincides with the Davisian hypothesis (Davis, 1899) of a uniform wearing of the earth's surface due to diffusion processes of soil movement.

However, the results of this experiment are somewhat counterintuitive if considered by themselves. If the erosional patterns of this experiment were indicative of long-term erosion rates, one would expect a much different morphology than that currently present: channels would be considerably more entrenched than they currently are (Figures 9 and 10). There are obviously diffusive erosion processes occurring that have maintained the smooth surface that is currently present. The only plausible explanation is that tillage and water-induced diffusive erosion must have played a major role in defining the landscape morphology of this watershed. Govers

et al. (1996) found a similar result for two agricultural fields in the UK. It will be interesting to see how cropped watersheds change in shape in the future under reduced and no-till conditions that are common now in the United States and other parts of the world; or alternatively, how the land will be managed to maintain more or less the current, relatively smooth morphological state that is conducive to modern farming techniques.

Most process-based soil erosion models use a rill/interrill approach, either explicitly as for the WEPP model (Nearing *et al*., 1989) and EuroSEM (Morgan *et al*., 1998) models, or implicitly as for the Griffith University Erosion System Template (GUEST) model (Rose *et al*., 1998). In these models sediment that is generated by sheet flow under the influence of raindrop impact is carried down the slope by rills, along with sediment scoured in the rills themselves. As such, these models do represent the water erosion process that was observed in this study, which was the long-distance, longitudinal transport of sediment generated form upper regions of the watershed (e.g., the toeslope deposition observed in Figure 6). However, the models have no mechanism for representing the diffusive erosion that was observed by the deposition of tracer in areas adjacent to source regions. To the extent that the diffusive erosion was caused by tillage, a tillage erosion model may be used. It may be, also, that water erosion models should have a diffusion component to better represent sheet flow. Studies similar to this, conducted in the absence of tillage, could clarify the relative contributions of tillage and water erosion to diffusive movement of sediment.

REFERENCES

Brakensiek LD, Osborn HB, Rawls WJ. 1979. *Field Manual for Research in Agricultural Hydrology*. Agriculture Handbook 224. US Department of Agriculture.

Brown RB, Cutshall NH, Kling GF. 1981 Agricultural erosion indicated by Cs-137 redistribution. II. Estimation of erosion rates. *Soil Science Society of America Journal* **45**: 1191–1197.

Daniels RB, Gilliam JW, Cassel DK, Nelson LA. 1985. Soil-erosion class and landscape position in the North Carolina Piedmont. *Soil Science Society of America Journal* **49**(4): 991–995.

Davis WM. 1899. The geographical cycle. *Geography Journal* **14**: 478–504.

De Roo APJ, Walling DE. 1994. Validating the ANSWERS soil erosion model using ^{137}Cs. In *Conserving Soil Resources: European Perspectives*, Rickson RJ (ed.). CAB International: Cambridge, UK; 246–263.

Ferro V, Di Stefano C, Giordano G, Rizzo S. 1998. Sediment delivery process and ^{137}Cs spatial distribution in a small Sicilian basin. *Hydrological Processes* **12**(5): 701–711.

Gamma Design Software. 2000. *GS$^+$ Geostatistics for the Environmental Sciences: Users Guide*, Version 5. Gamma Design Software: Plainwell, MI.

Govers G, Quine TA, Desmet PJJ, Walling DE. 1996. The relative contribution of soil tillage and overland flow erosion to soil redistribution on agricultural land. *Earth Surface Processes and Landforms* **21**: 929–946.

Hussain I, Olson KR, Jones RL. 1998. Erosion patterns on cultivated and uncultivated hillslopes determined by soil fly ash contents. *Soil Science* **163**: 726–738.

Kelley GE, Edwards WM, Harrold LL, McGuinness JL. 1975. *Soils of the North Appalachian Experimental Watershed*. Misc. Publication No. 1296. Agricultural Research Service, US Government Printing Office: Washington DC.

Montgomery JA, Busacca AJ, Frazier BE, McCool DK. 1997. Evaluating soil movement using Cesium-137 and the Revised Universal Soil Loss Equation. *Soil Science Society of America Journal* **61**: 571–579.

Morgan RPC, Quinton JN, Smith RE, Govers G, Poesen JWA, Auerswald K, Chisci G, Torri D, Styczen ME. 1998. The European Soil Erosion Model (EUROSEM): a dynamic approach for predicting sediment transport from fields and small catchments. *Earth Surface Processes and Landforms* **23**: 527–544.

Nearing MA, Foster GR, Lane LJ, Finkner SC. 1989. A process-based soil erosion model for USDA–Water Erosion Prediction Project technology. *Transactions of ASAE* **32**: 1587–1593.

Olson KR, Gennadiev AN, Jones RL, Chernyanskii S. 2002. Erosion patterns on cultivated and reforested hillslopes in Moscow Region, Russia. *Soil Science Society of America Journal* **66**: 193–201.

Penck W. 1924. *Die Morphologische Analyse*. J. Englehorn's Nachfolger: Stuttgart (English translation by Czech H, Boswell KC, 1953, St Martin's Press: New York).

Polyakov VO. 2002. Use of rare earth elements to trace soil erosion and sediment movement. PhD thesis, Purdue University, Department of Agronomy.

Polyakov VO, Nearing MA. 2004. Rare earth element oxides for tracing sediment movement. *Catena* **55**: 255–276.

Quine TA. 1999. Use of ceasium-137 data for validation of spatially distributed erosion models: the implication of tillage erosion. *Catena* **37**: 415–430.

Quine TA, Govers G, Walling DE, Zhang X, Desmet PJJ, Zhang Y. 1997. Erosion processes and landform evolution on agricultural land: new perspective from cesium-137 data and topographic-based erosion modeling. *Earth Surface Processes and Landforms* **22**: 799–816.

Ritchie JC, McHenry JR. 1990. Application of radioactive fallout cesium-137 for measuring soil erosion and sediment accumulation rates and patterns: a review. *Journal of Environment Quality* **19**: 215–233.

Ritchie JC, Spraeberry JA, McHenry JR. 1974. Estimating soil erosion from the redistribution of fallout ^{137}Cs. *Soil Science Society of America Proceedings* **38**: 137–139.

Rose CW, McCallan ME, O'Leary BM, Sander G. 1980. Testing a model of field-scale soil erosion and deposition on a plane land element using the fallout isotope ^{137}Cs. In *Proceedings of the Conference on Agricultural Engineering*, Geelong, Institute of Engineers, Australia, Reprint of Papers no. 80/7.

Rose CW, Coughlan KJ, Fentie B. 1998. Griffith University Erosion System Template (GUEST). pp. 399–412. In Boardman J, Favis-Mortlock DT (eds). *Modeling Soil Erosion by Water*. NATO-ASI Global Change Series, Springer: Heidelberg.

Sidorchuk AJ, Golosov VN. 1996. Calibration of soil-erosion models based on study of radioactive fallout. *Eurasian Soil Science* **28**(10): 383–395.

Sutherland RA. 1994. Caesium-137 soil sampling and inventory variability in reference locations: a literature survey. *Hydrological Processes* **10**(1): 43–53.

Takken I, Bueselinck L, Nachtergaele J, Govers G, Poesen J, Degraer G. 1999. Spatial evaluation of a physically-based distributed erosion model (LISEM). *Catena* **37**: 431–447.

USEPA. 1995. *Test Methods for Evaluating Solid Waste – SW846*, update III (3rd edn). US Government Printing Office: Washington, DC.

Van Muysen W, Govers G. 2002. Soil displacement and tillage erosion during secondary tillage operations: the case of rotary harrow and seeding equipment. *Soil and Tillage Research* **65**(2): 185–191.

Van Oost K, Govers G, Van Muysen W. 2003. A process-based conversion model for caesium-137 derived erosion rates on agricultural land: an integrated spatial approach. *Earth Surface Processes and Landforms* **28**(2): 187–207.

Zhang XC, Fredrich JM, Nearing MA, Norton LD. 2001. Potential use of Rare Earth oxides as tracers for soil erosion and aggregation studies. *Soil Science Society Journal* **65**: 1508–1515.

Zhang XC, Nearing MA, Polyakov VO, Friedrich JM. 2003. Using rare earth oxide tracers for studying soil erosion dynamics. *Soil Science Society Journal* **65**: 1508–1515.

